

PTFE as a viable sealing material for lightweight mass spectrometry ovens in dusty extraterrestrial environments

Feergus A. J. Abernethy¹,^{ORCID} Hannah Chinnery,¹ Robert Lindner² and Simeon J. Barber¹

¹Planetary & Space Sciences, School of Physical Sciences, The Open University, Walton Hall MK7 6AA, UK

²European Space Agency, ESA-ESTEC, Keplerlaan 1, NL-2200 AG, Noordwijk ZH, the Netherlands

Accepted 2024 January 21. Received 2024 January 10; in original form 2023 October 10

ABSTRACT

Ever increasing interest in the Moon, not only for scientific but also commercial and prospecting purposes, requires a more streamlined and reproducible approach to issues such as the sealing of sample handling ovens, in contrast to the mission-specific mechanisms which have tended to prevail in the past. A test breadboard has been designed and built in order to evaluate the leak rates of different oven sealing concepts and materials within the context of the PROSPECT Sample Processing and Analysis (ProSPA) instrument being developed for the European Space Agency. Sealing surface geometries based on a simple 90° knife-edge, and two widely used vacuum fitting standards (VCR® and ConFlat®) have been tested using PTFE (polytetrafluoroethylene) gaskets in vacuum across a temperature range of –100 to 320°C, equivalent to a projected –100 to 1000°C sample heating range in the ProSPA ovens. The impact of using glass- and carbon-filled PTFE has also been investigated, as has the effect of dust coverage of JSC-1A lunar simulant up to 9 per cent by area. The best combination of properties appears to be unfilled PTFE, compressed between two 90° knife-edges with a confining force of ~400 N. This can produce a leak rates within the 10^{–7} Pa m³ s^{–1} range or better regardless of the level of dust applied within the experimental constraints. A strong temperature-dependence on the leak rate is identified, meaning that careful oven design will be required to minimize the temperature at the seal interface even within the operational temperature range PTFE itself.

Key words: Instrumentation – Mass Spectrometry – Lunar – ISRU.

1. INTRODUCTION

In recent years there has been a substantial increase in activities targeting the Moon, with all major space agencies planning new exploration programmes, as well as the increasing involvement of private companies, many of which are developing their own launch assets. The primary drivers for this renewed interest are investigations into the availability of water in the lunar regolith (e.g. Li & Milliken 2017; Lin et al. 2022) and *in situ* resource utilization (ISRU), ostensibly to provide a lunar infrastructure that can serve to support long-term human presence and as a relay for crewed missions to Mars, itself a target of extensive investigation. Many of these activities require the use of high temperatures, either for extraction of volatile species as part of sample analysis through mass spectrometry, as performed in terrestrial lab analysis on lunar samples (e.g. Mortimer, Verchovsky & Anand 2016) or comparable activities on other bodies (Goesmann 2007; Morse et al. 2009), or for processing reactants as part of an ISRU investigation such as the reduction of ilmenite to produce water (e.g. Sargeant et al. 2021). Generally, the most effective way of performing such analyses in extraterrestrial environments is to seal the sample within a refractory crucible and heat it using an attached heating element to make a sample oven. An example of such an oven design is shown in Fig. 1. This process is reliant on effective seals to prevent the

escape of sample and reactant gases leading to reduced yields in the case of ISRU and isotopic fractionation effects in the case of isotopic analysis. While sealing these types of system is relatively straightforward to achieve on Earth, systems designed to operate on the Moon or Mars are rendered more challenging by the need for full automation, lower power availability, and mass constraints. Further complications arise from the presence of dust, particularly on the Moon, where the pervasive nature of the highly abrasive, electrostatically charged angular fragments of glass and rock that make up the lunar regolith are well noted (e.g. Colwell et al. 2007; Grün, Horanyi & Sternovsky 2011).

The problem of sealing samples in space is not new, and there are many examples of sealing mechanisms that have been produced for specific missions over the last few decades. At the smaller scale, there have been low mass options such as the systems used in the COSAC (Goesmann 2007) and Ptolemy (Wright et al. 2007; Morse et al. 2009) instruments on Rosetta, consisting of platinum crucibles sealed by a spherical ZrO₂. At the other end of the scale there are large, complex, and heavy drilling and subsampling mechanisms such as those used in the Curiosity (Kennedy et al. 2006; Mumm et al. 2008; Anderson et al. 2012), Perseverance (Moeller 2020), and upcoming ExoMars (Richter et al. 2015) rovers. Each of these requires a significant compromise, either sealing efficiency in the case of the Rosetta examples, or mass and cost in the case of the Mars rovers. Given the widespread interest in lunar exploration, and the repetition of discussions regarding dust mitigation, it is useful to

* E-mail: feergus.abernethy@open.ac.uk

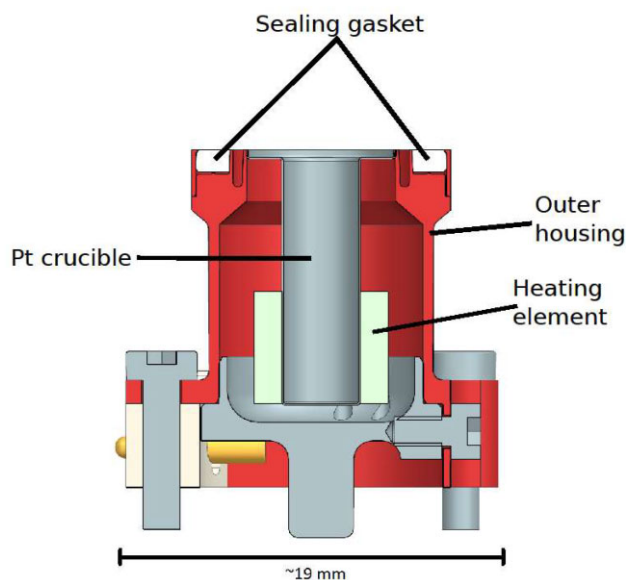


Figure 1. Cross-section Computer-Aided Design (CAD) schematic of the ProSPA oven design.

work towards a standardized sealing design for small-scale extraction ovens.

European Space Agency PROSPECT (Package for Resource Observation and in-Situ Prospecting for Exploration, Commercial exploitation, and Transportation) is an ideal candidate to base such an activity on. A subset of this system, termed ProSPA (PROSPECT Sample Processing and Analysis) is a miniaturized chemical laboratory designed for both chemical extraction and basic prospecting ISRU experiments (Barber et al. 2018). The ovens are designed to have a high thermal gradient between the sample and the outer structure in order to allow a wide range of sealing gaskets to be used. The system is designed to be flexible and reproducible, meaning it is easily incorporated into any instrument package and providing the potential to test any sealing concepts thoroughly in operational environments.

2. SYSTEM DESIGN

We previously investigated the ability of soft metal (indium) and perfluoroelastomer (Kalrez®) gaskets to seal against a knife-edge with a dust load present (Abernethy, Sheridan & Barber 2020). As part of this, a method was identified to make the sealing environment more representative of lunar conditions. For this work, a completely new system was developed, termed as Environmental Sealing Breadboard (Fig. 2). This consists of a box vacuum chamber, which hosts an interchangeable dummy oven with a knife-edge profile set within a thermally controlled stage (cross-section shown in Fig. 3). A ballscrew-driven linear actuator with a compressible bellows is used to translate vertical motion into the chamber, driving a rod (Fig. 3) to allow the system to interface and disengage from the ovens without breaking vacuum. The rod incorporates a set of dome washers to allow spring tension to compensate for material creep in the tested gasket material. In the lower section of the rod the construction changes from solid stainless steel to VCR® vacuum components, with the tip consisting of an interchangeable knife-edge machined from a bored $\frac{1}{4}$ " VCR® blind gland. A T-piece permits the connection of a gas line through a feedthrough on the chamber to allow the internal volume to be pressurized with helium for leak testing during experiments.

The system is connected to a variety of measurement devices. A Burster 8431 vacuum-compatible miniaturized load cell, built into the force application rod, is used to constantly monitor the force applied by the linear actuator. Measurement of applied gas pressure within the sealed volume is accomplished using an MKS Instruments type 722B capacitance manometer with a 5000 Torr (~ 6.6 bar) full scale, while the helium leak is measured using a calibrated Hiden HALO 200 quadrupole RGA (Residual Gas Analyser). Alternatively, an MKS type 627F temperature-regulated capacitance manometer with a 0.02 Torr (0.03 mbar) full scale can be used to measure the general chamber rise rate over time. Temperature regulation of the stage was achieved using a Eurotherm 3216 PID (Proportional - Integral - Derivative) controller to balance heating, using a 500 W cartridge heater embedded in the stage, and a liquid nitrogen-chilled flow of dry compressed air through a sealed coil of 6 mm diameter copper pipe surrounding the stage. The cartridge heater voltage was restricted to 100 Vac to prevent electrical discharge effects in the vacuum. This resulted in an operational temperature range for the stage of ~ -100 to $+350^\circ\text{C}$, as measured by a type K thermocouple embedded within the stage as near as possible to the oven mounting point and encompassing the predicted operational range of the ProSPA ovens. An additional three type K thermocouples were used to monitor heat conduction through the metalwork of the chamber, and to ensure that the load cell remained within its operational temperature range.

Vacuum on the system was maintained through two separate pumping lines, for the main chamber and the leak measurement system, respectively. Both sections were pumped using Pfeiffer HiCube 80 pumping stations with an additional MVP 020–3 diaphragm pump for rough pumping of the chamber from atmosphere. Ultimate vacuum at room temperature was 1×10^{-5} mbar for the chamber section and 5×10^{-8} mbar for the measurement section.

3. MATERIALS AND METHODS

Although both indium and Kalrez® were found to be viable sealing materials under dust loading (Abernethy et al. 2020), these results were limited. During these experiments, testing was only performed with a knife-edge sealing a single side of the gasket surface, in contrast to the two-sided knife-edge sealing proposed for the ProSPA ovens. When tested under more operationally relevant conditions, it was found that the sealing force was sufficient to cut through the Kalrez gaskets, making them unsuitable. Indium was also deemed to be unsuitable on the basis of the significant limitations imposed by its low melting temperature. PTFE was ultimately selected for the baseline testing due to its similar temperature profile to the originally baselined Kalrez.

A further limitation was that of reproducible dust loads. Here, this was achieved through the use of a PALAS RBG 1000 dust aerosolization unit. JSC 1A (Liu & Taylor, 2011) was again selected for the testing as a result of its availability and well characterized nature (Arslan et al., 2010; Hill et al., 2007; LaMarch et al., 2011; Ray et al., 2010), although in this instance it was sieved to 100 μm due to the limitations of the RBG 1000. Brush speed of 800 rpm, a 200 mm h^{-1} feed rate, and a 1 bar (above atmosphere) gas pressure for 20 s was sufficient to grade a sample tray of $\sim 18 \times 30$ cm from ~ 2 – 9 per cent surface coverage of dust. This was measured by using a luxmeter to take obscuration measurements of transmitted light through glass witness slides that were interspersed with the PTFE gaskets.

The sealing experiments and data collection were all handled by LabVIEW scripts, ensuring that the experimental protocol could be kept consistent for every run. The software included a subroutine for checking and correcting for creep and thermal expansion/contraction

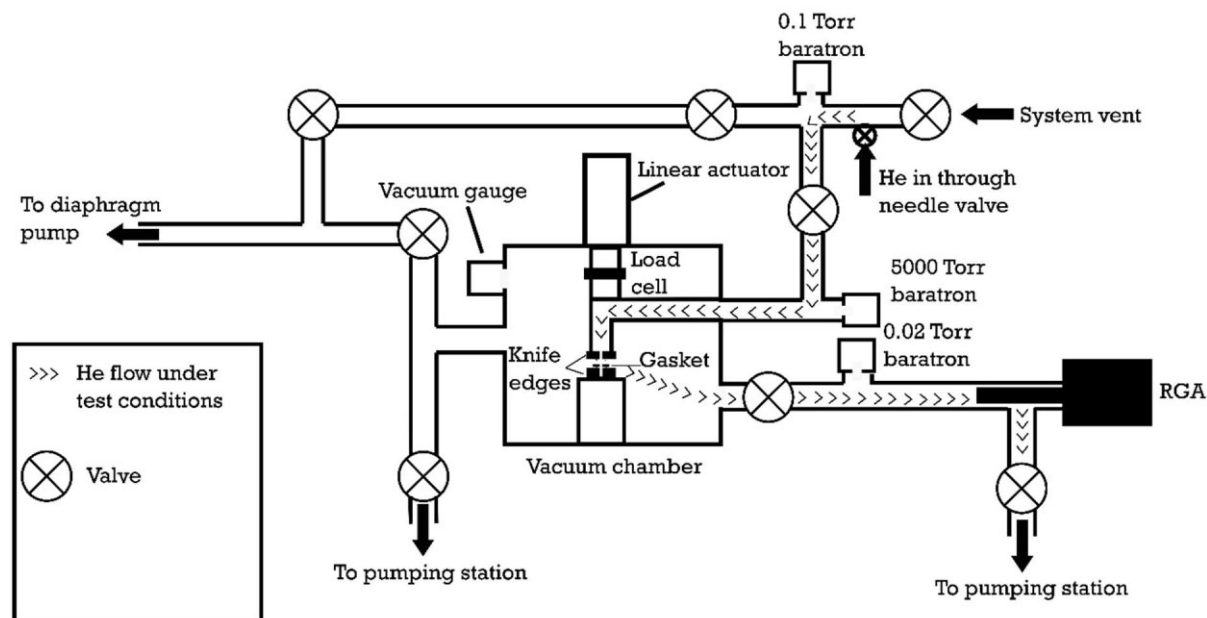


Figure 2. Schematic of the Environmental Sealing Breadboard.

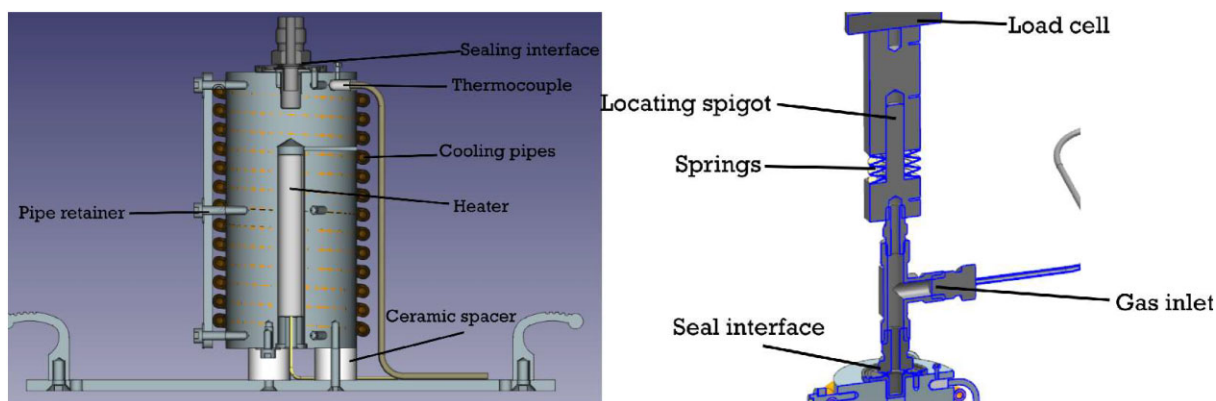


Figure 3. CAD cross-section models of the heated stage (left panel) and the force application rod (right panel).

in the gasket material and ensuring that the confining force was always within ~ 5 N of the set value. An experiment building section allowed for both multiple sealing events with variable force, with complete disengagement between each event, and a confined heating mode to simulate reuse of the gasket and heating of a confined sample, respectively. Every temperature step in the list was executed before moving on to multiple sealing events if required. The software sequence initialized with a heat ramp to the starting temperature. Once this was reached, the force specified in the experimental set-up was applied and a valve was opened to pressurize the sealed volume to ~ 2 bar pressure with respect to the vacuum system. The chamber and measurement sections were then isolated from the pumps and the chamber rise rate was determined using the 0.02 mTorr baratron. The sections were subsequently isolated from one another again, pumped, and 10 measurements of $m/z = 4$ were taken using the RGA in order to determine the background of He in the system. With the pump to the chamber once again isolated, the valve between the measurement and chamber sections was opened to allow for dynamic flow through

the RGA. This was permitted to flow for 5 min in order to equilibrate, after which 100 measurements were taken on the RGA to determine the helium flow through the seal. After measurement was completed, the sections were again isolated from one another and pumped before moving on to the next temperature. The seal was not broken during individual heating ramps. For the tests, dust levels were selected at 0, 2, 5, and 9 per cent (limited by the maximum reproducible dust loading in the sample tray). Three different sealing geometries were used; a 90° symmetrical knife-edge, and two styles based on standard vacuum fittings (VCR[®] face seal fittings and CF[®] knife-edges). These are shown in Fig. 4. Three different compositions of PTFE were also tested, consisting of standard PTFE, glass-filled PTFE, and carbon-filled PTFE. The filled compositions were filled to 40 per cent by mass. As a result of the large number of test permutations that these variations represent, and the desire to find the most effective combination, the tests were carried out in stages with activity ceasing on certain permutations if they did not perform well at a certain level or if there was little difference between them and the baseline case.



Figure 4. Knife-edge profiles used in the tests. Descending surface (top panel) is based on a modified 1/4" VCR blanking plug. L-R on both rows: 90°, VCR®, and CF®.

4. RESULTS

4.1 Clean tests

The first set of tests was carried out to determine the effectiveness of the various knife-edge geometries on the sealing performance. A 400 N sealing force was chosen in order to replicate that available from the ProSPA tapping station. Results for the three different knife-edge styles can be seen in Fig. 5. Ten repeat experiments were performed for each of the VCR®- and CF®-style knife-edges, and nine repeats were performed for the 90° knife-edge. The most obvious point to note is the presence of a trend of increasing leak rate as the temperature rises. In the case of the 90° knife-edge, this is a broadly linear trend starting at leak rates in the high 10^{-8} or low 10^{-7} $\text{Pa m}^3 \text{s}^{-1}$ range and progressing towards leak rates of $\sim 1.0 \times 10^{-6}$ $\text{Pa m}^3 \text{s}^{-1}$ by 320°C (the maximum temperature used). The CF®-style knife-edge trend appears similar up to $\sim 220^\circ\text{C}$, at which point the leak rates start to increase exponentially towards the upper reaches of the 10^{-6} $\text{Pa m}^3 \text{s}^{-1}$ range. The VCR-style knife-edge, in contrast, seems to experience a very similar degradation to that of the 90° but does not appear to perform reliably at lower temperatures. As the temperature goal for sealing operability for this work was -100°C , this means that there was sufficient doubt about the performance of the VCR edge at lower temperatures to eliminate it and use the baseline 90° edge for further testing.

4.2 PTFE variations

As a result of the consistent trend towards higher leak rates at higher temperatures using plain PTFE, a second series of tests was conducted on PTFE with different fill compositions. The reasoning was that the increased rigidity of the gasket caused by the fill may serve to reduce ongoing material creep after the initial deformation of the gasket and thus improve the seal. The results of these tests are compared with the 90° knife-edge tests from Fig. 5. Each filled composition test was performed 10 times.

It is clear from the results in Fig. 6 that the impact of temperature on the leak rates of the glass-filled composition is significantly reduced. However, the leak rates themselves are both highly variable between different test runs and significantly worse, at between 2.3×10^{-6} and 1.2×10^{-5} $\text{Pa m}^3 \text{s}^{-1}$, than the rates experienced by either the plain or carbon-filled PTFE. Carbon-filled PTFE is comparable with the plain composition at the higher temperature ranges (maximum leak rate of 2.0×10^{-6} $\text{Pa m}^3 \text{s}^{-1}$ for plain PTFE versus 2.7×10^{-6} $\text{Pa m}^3 \text{s}^{-1}$ for carbon-filled) and is more consistent across the full range. But again, the overall leak rates at the lower temperatures are worse than the baseline case, at between 1.6×10^{-7} and 4.6×10^{-7} $\text{Pa m}^3 \text{s}^{-1}$ for carbon-filled as opposed to $< 2.0 \times 10^{-7}$ $\text{Pa m}^3 \text{s}^{-1}$ for all 20°C steps when using plain PTFE. Based on these results, there was no benefit to using filled compositions.

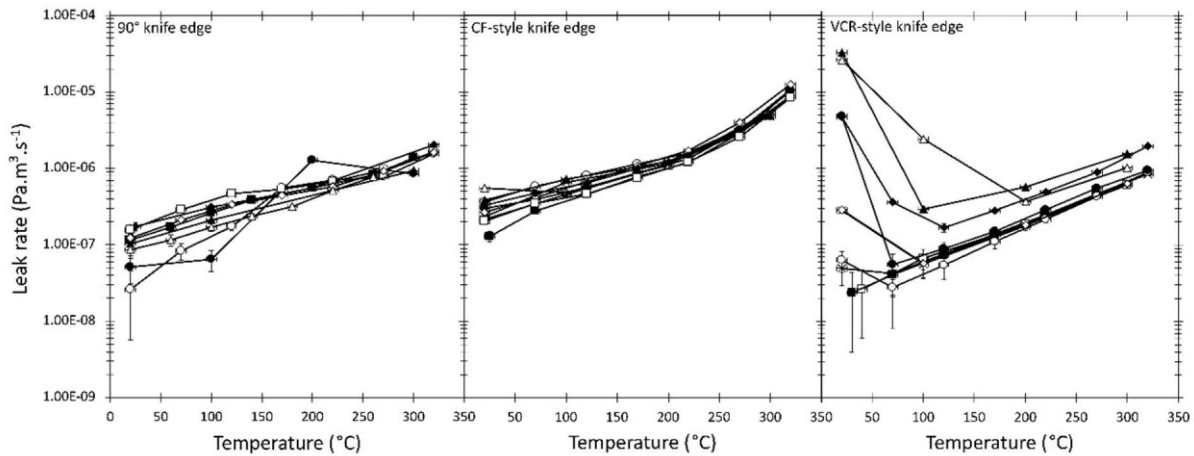


Figure 5. Clean PTFE seal results for the three different knife-edge options. The 90° knife-edge experiment was performed nine times with the CF® and VCR® knife-edges performed 10 times each. Uncertainties are $\pm 5^\circ\text{C}$ on the temperature measurement, on the basis of uncertainty of the temperature at the exact time the leak rate was measured rather than problems with the accuracy of the Eurotherm controller. Uncertainties on the leak rate measurement are derived from the RGA reproducibility during calibration and are $2 \times 10^{-8} \text{ Pa m}^3 \text{ s}^{-1}$ (2σ).

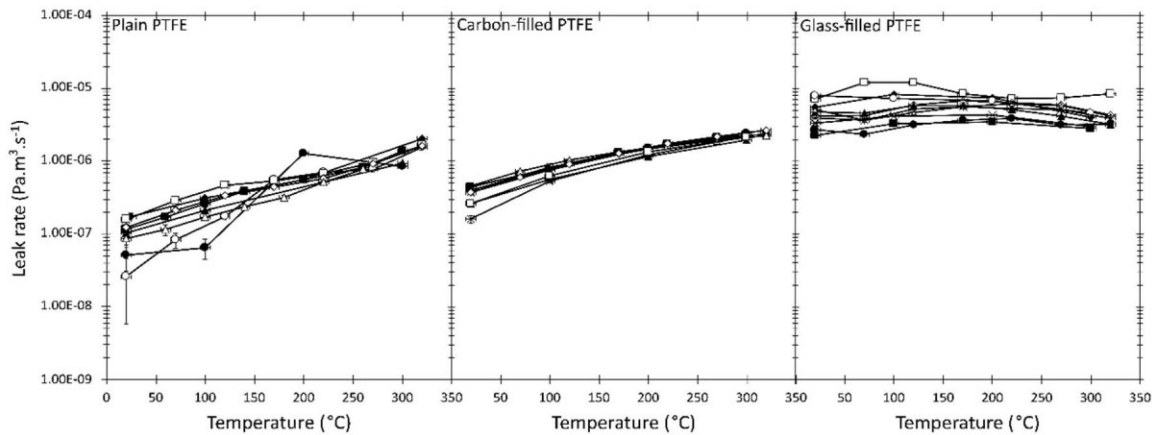


Figure 6 Clean PTFE of varying compositions tested using the 90° knife-edge. Uncertainties are 5°C and $2 \times 10^{-8} \text{ Pa m}^3 \text{ s}^{-1}$ (2σ) for the temperature and leak rate, respectively.

4.3 Dust loading

Given the performance comparisons outlined above, the dust loading experiments were performed solely with the 90° knife-edge into a plain PTFE gasket of 1 mm thickness. The dust loads used were 0, 2, 5, and 9 per cent as measured by obscuration on glass witness slides present during the dust loading procedure. Nine experiments were performed using 0 and 9 per cent obscuration, 12 were performed using 2 per cent, and 10 on the 5 per cent obscuration samples. The results are compared in Fig. 7.

While the data do show that adding dust to the seal surface does increase the chances of a failure to seal during the initial phase, there is no systematic evidence to suggest that increasing the dust levels increases the probability of failure. It is also clear that this failure only occurs during the first temperature step in all but one case. Even in the cases where the gasket seals successfully immediately there is a slight elevation in the leak rates. Dust-free samples consistently experience leak rates of $<2.0 \times 10^{-7} \text{ Pa m}^3 \text{ s}^{-1}$ at room temperature and can reach rates of as low as $2.6 \times 10^{-8} \text{ Pa m}^3 \text{ s}^{-1}$ in the best case. There are one or two outlying examples clearly in $10^{-8} \text{ Pa m}^3 \text{ s}^{-1}$ range in the dusty samples, but the bulk of the data fall into the low $10^{-7} \text{ Pa m}^3 \text{ s}^{-1}$ range. There does not seem to be a significant

difference between the different dust loads either in the impact of temperature on the leak rates or the ultimate leak rate at $\sim 300^\circ\text{C}$. In fact, it appears that the dusty gaskets generally perform slightly better at higher temperatures, showing worst-case leak rates of $\sim 5 \times 10^{-7} \text{ Pa m}^3 \text{ s}^{-1}$, less than the clean PTFE.

4.4 Cold tests

The lack of significant difference between the leak rates within the determined ranges meant that the cold tests could be performed as a simple comparison between clean PTFE and that exposed to the largest amount of dust. Nine clean gaskets were tested and compared with five dust contaminated gaskets. Sample availability meant that only two gaskets were available with 9 per cent dust loading, so the remaining three were performed at 7 per cent. An overview of the full data set, separated into clean and dusty gaskets, is shown in Fig. 8.

At temperatures greater than -50°C , the data appear to follow the same trend as those started under room temperature conditions, including a continuing regression to better leak rates as the gasket is cooled. This ultimately results in measurements of better than $1.0 \times 10^{-8} \text{ Pa m}^3 \text{ s}^{-1}$, although the measurement uncertainty

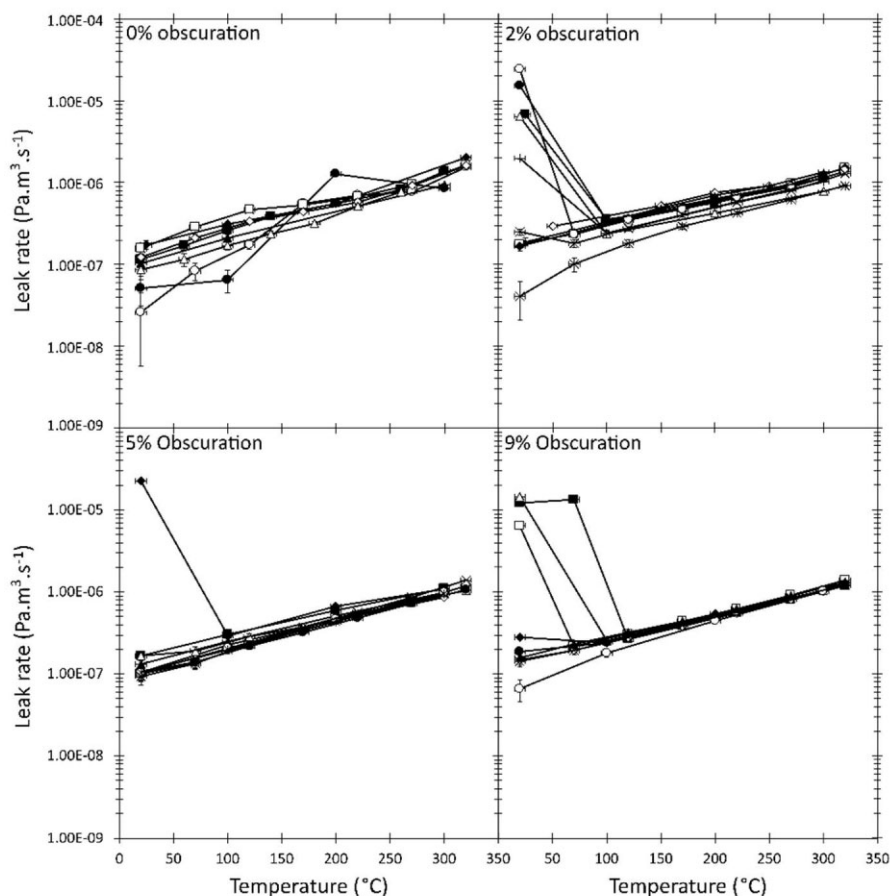


Figure 7. Leak rate results from different dust loads on plain, 1 mm thick PTFE compressed between 90° knife-edges. The 0 per cent obscuration samples are the same as the 90° and plain PTFE results shown in Figs 5 and , respectively. Uncertainties are 5°C on the temperatures, to account for uncertainties as to the exact temperature when the measurement was made, and $2 \times 10^{-8} \text{ Pa m}^3 \text{ s}^{-1}$ (2σ) on the leak rate.

becomes substantial at these leak rates. More obvious, however, is the poor performance of the gaskets at the lowest temperatures of -80 to -100°C , reaching into the $10^{-5} \text{ Pa m}^3 \text{ s}^{-1}$ range in some cases. A comparison between clean and contaminated samples demonstrates that poor performance was not restricted to the contaminated gaskets. A further division of the contaminated gaskets into the 7 and 9 per cent obscuration does appear to show better cold performance from the lower dust load, but the data are not sufficient for this to be conclusive.

5. POST SEAL INDENTS

Post analysis, 10 samples were sent to TaiCaan Technologies Ltd for analysis using their XYRIS 2020 H white light imaging systems. Surface position points were taken with $10 \mu\text{m}$ spacings on a $13 \times 13 \text{ mm}$ grid and used to generate a co-ordinate point cloud, allowing the surface of the gasket to be reconstructed. These data were then processed using TaiCaan's BEX software package to analyse the knife-edge indent depths.

Imaging of the surfaces revealed that there was a significant amount of distortion of the gasket due to the sealing procedure, although whether this was the result of the initial sealing procedure, or the withdrawal of the knife-edge is uncertain. There was also significant thinning of the material in the active sealing region (Fig. 9), to the extent of causing ruptures in some samples. There

was no correlation between samples that ruptured during the sealing process and those that performed poorly in terms of leak rates. Across the gaskets analysed, knife-edge penetration depths varied in the range of ~ 100 – $500 \mu\text{m}$ on the upper surface and ~ 160 – $300 \mu\text{m}$ on the lower surface with no obvious correlation to sealing performance.

6. DISCUSSION

The results consistently show a strong correlation between the sealing performance and the temperature. The most logical explanation for this would have been increased temperature causing a rise in gas pressure inside the sealed volume. This is not the case however, as the pressure was monitored throughout the course of each experiment and re-equilibrated at each step to avoid such an outcome. Some pressure changes were inevitable as a result of gas lost through leakage and through thermal expansion, but the latter was generally found to be $< 100 \text{ mbar}$, less than 5 per cent of the target pressure given that the experimental pressure generally exceeded 2 bar. This variation is considered insufficient to have caused a leak rate increase of 2 orders of magnitude across the 400°C temperature range, consistent with what is observed in some of the cold experiments. A more compelling explanation lies in the mechanical properties of PTFE, specifically its tendency to creep. Various authors have observed the effects of temperature on the strain observed in PTFE gaskets under compression (e.g. Rae & Dattelbaum 2004; Zheng

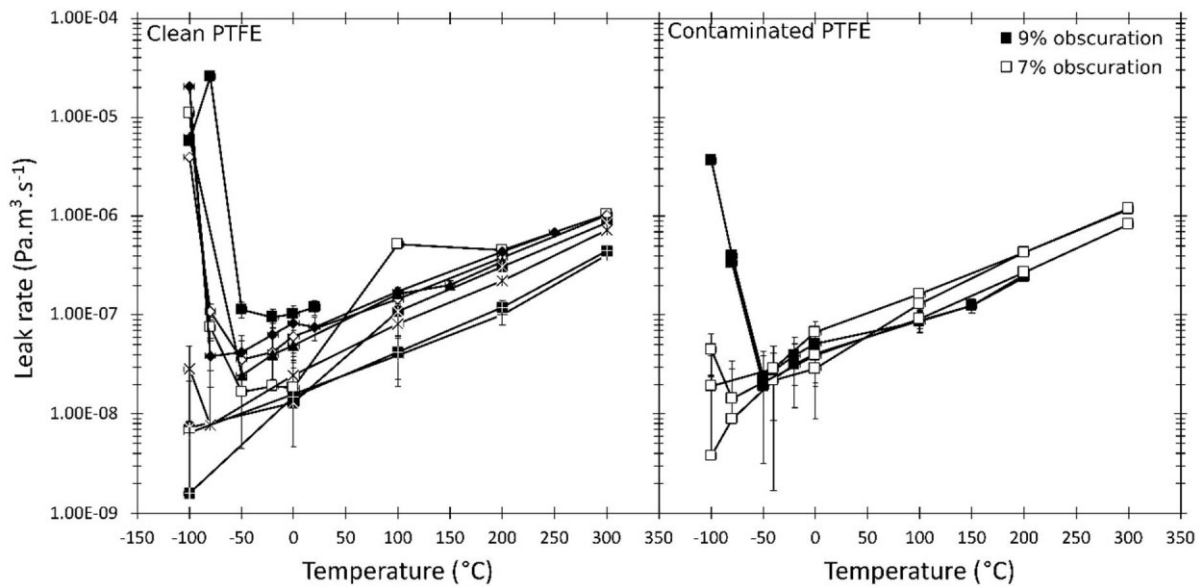


Figure 8. Separated data from the PTFE cold sealing tests.

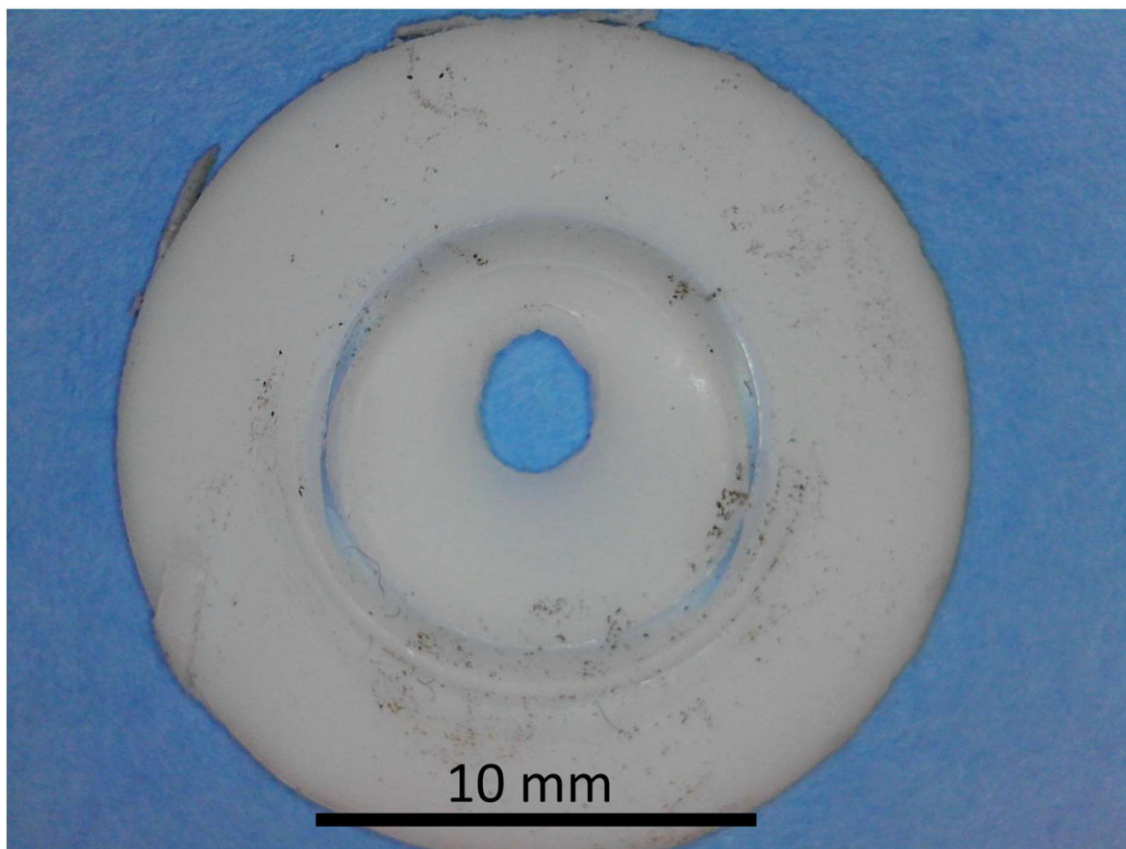


Figure 9. Post-seal gasket showing distortion of the centre hole and the remnants of the dust coating. Some indented areas have been thinned to transparency but in this example the gasket has not ruptured.

et al. 2017) and measured the mechanical rigidity under different temperature conditions (Rae & Dattelbaum 2004; Bergström & Hilbert 2005; Calleja et al. 2013). While a detailed discussion of the mechanical properties of PTFE are well beyond the scope of this paper and the expertise of the authors, the consensus appears

to be that of a decreased rigidity (Bergström & Hilbert 2005) leading to greater strain effects under higher temperatures (Rae & Dattelbaum 2004; Zheng et al. 2017). Specific phase transitions in the crystal structure are also noted (McCrum 1959; Rae & Dattelbaum 2004; Calleja et al. 2013) at various temperatures. Such changes,

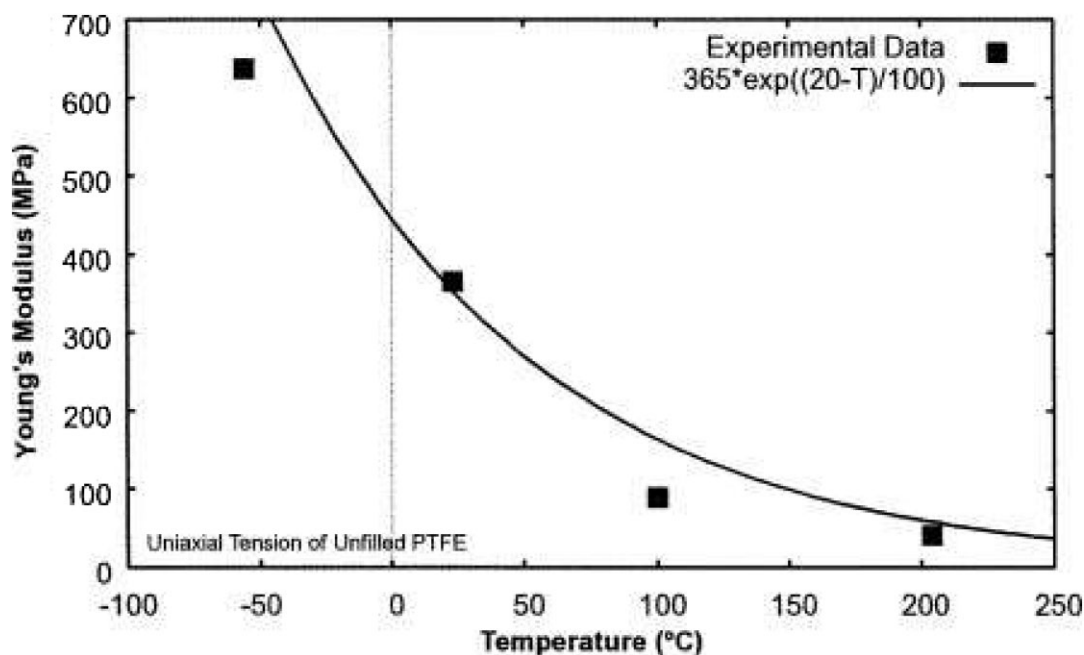


Figure 10. Graph of temperature versus Young's modulus for PTFE (Bergstrom & Hilbert 2005).

through disrupting the structure of the PTFE and creating areas of amorphous material, are likely to increase the diffusivity of gases through the material, as observed by Pasternak, Christensen & Heller (1970) and Sebök et al. (2016). The impact of molecular size on diffusivity (Matteucci et al. 2006) means that helium, as used in these tests, will be particularly susceptible. This also means the species of interest for ProSPA, being larger molecules, are likely to experience lower leak rates and a smaller negative impact from elevated temperatures than those observed here, although the effects of the gas solubility of species such as CO₂ and the effects of gas mixtures as opposed to predominantly pure gases (Sebök et al. 2016) will make this relationship quite complex. However, this is not ideal for the execution of ISRU experiments during lunar operation involving the use of hydrogen, such as the static ilmenite reduction experiments outlined by Sargeant et al. (2021). In this case the diffusivity of hydrogen, comparable with that of helium, and the high temperatures and pressures required for the reaction may be capable of causing significant loss of reactant gases during the experiment. This is not critical as the ISRU extraction experiments are not reliant on preserving abundances or isotope ratios of evolved gases and, as such, a greater level of loss can be tolerated. None the less, this will be an important point to consider when planning volumes of reactant gases to carry with payloads and in inferring the presence or absence of a reaction based on feedback from pressure sensors. It would be possible to minimize the effect by further impeding the heat transfer from the oven crucible to the seal, allowing the seal to operate at lower temperatures, but this has the potential to impose further severe complexities on an already complex oven design.

Another critical issue to understand is the poor leak performance that is intermittently experienced by the seal gaskets as they approach the minimum temperatures used in these experiments. The temperature-dependent leak rate appears to operate as described above until a temperature of -80 to -100°C is reached, at which point the seal quality can degrade significantly. This is consistent with the proposed glass transition temperature of PTFE at approximately -100°C suggested by McCrum (1959) and supported experimentally

by data from Rae & Dattelbaum (2004) and Calleja et al. (2013). Modelling and experimental work performed by Bergström & Hilbert (2005) also shows a rapid increase in the Young's modulus of PTFE with decreasing temperature, demonstrating a change in the material properties to a more brittle and rigid quality. This is reproduced in Fig. 10. The results from Bergström & Hilbert (2005) only have a minimum temperature of -50°C , but the behaviour and trends at this temperature mean that we are comfortable inferring a continued trend to the relevant temperatures. The data presented herein show that there does not appear to be any statistically relevant preference for whether the clean or dust-loaded gaskets perform poorly at these temperatures. While there is some suggestion that there is a difference between the 7 and 9 per cent dust loads, the data are insufficient to verify this, and it does not explain why the clean gaskets are equally likely to experience this effect. It therefore appears likely that the intermittent poor performance is solely the result of the reduced deformability of the gaskets themselves. It is possible that minor misalignments could occur during the initial application of force to the gasket. These can be compensated for by deformation when the PTFE is sufficiently ductile, but when it is more brittle it would not be able to behave in the same way, resulting in knife-edge penetration that is insufficient to form a good seal. This means that any tapping station sealing into ovens with PTFE gaskets at temperatures close to or less than -100°C will need to be designed with high stability to ensure an even loading of the sealing force.

7. CONCLUSIONS

We have developed a representative lab scale breadboard of a tapping station, operating under vacuum conditions with a sealed internal volume pressurized to ~ 2 bar and an operational temperature range of -100 to 320°C . Using this system, we have determined that PTFE is a viable gasket material for mass spectrometry ovens on small-scale lunar prospecting and demonstration activities such as ProSPA. Using helium as a test gas, PTFE is capable of maintaining leak rates of $< 10^{-7}$ Pa m³ s⁻¹ within an operational temperature range of -100

to 320°C and with dust coverage of up to 9 per cent of surface area. The best performance has been achieved by compressing the gasket between two symmetrical 90° knife-edges, with other candidate profiles based on common vacuum sealing profiles, VCR® and ConFlat®, not performing to the same standard. It has also been determined that plain PTFE produces better leak rates than either glass-filled or carbon-filled compositions.

The use of PTFE is not without challenges, however. The structural changes that result from the heating and cooling of the material result in a strong correlation between temperature and leak rate, and variability on the level of approximately 2 orders of magnitude across the temperature range of the experiments. This has significant implications for interpretation of any analysis or experimental reactions involving highly diffusive gases such as hydrogen or helium, such as ilmenite reduction. Furthermore, it is likely that the glass transition of PTFE is within the temperature range of the experiments and operational requirements, requiring strong constraints on the alignment and precision of any tapping station to seal into PTFE, although such a seal is demonstrated to be possible. Finally, in order to use PTFE effectively in applications such as ProSPA, which require samples heated to 1000°C, the thermal design of the ovens is important in order to keep the PTFE seal within its operational range.

ACKNOWLEDGEMENTS

Dr Ady James and Amy Hyde are thanked for the editorial handling of this manuscript; a reviewer is thanked for their helpful suggestions for improvements to the manuscript. Darren Yau (DASTEC Consulting Ltd) is thanked for his assistance with the design and thermal modelling of the Environmental Sealing Breadboard. Andrew Chalmers and Filter Integrity Limited are thanked for their advice and loan of the PALAS RBG 1000 for dust loading. Other design and manufacturing work was performed by Dowding Precision Inc. and UHV design limited. White light imaging measurements were performed at TaiCaan Technologies Ltd by Dr Tom Bull. Many of these activities were performed during difficult periods resulting from COVID-19. Thus, particular thanks are reserved for the technical staff at The Open University School of Physical Sciences, specifically Thomas Webley, Lily Hills, and Elisabeth Moro, without whom this would not have been possible. This work was performed under contract 4000128701/19/NL/MG entitled ‘Improvement of Sample Containment/Handling for Volatile Analysis’ a project of, and funded by, the European Space Agency. Designs of the ProSPA ovens are reproduced with the permission of the ProSPA team, on the ESA-funded activity PROSPECT.

DATA AVAILABILITY

The data underlying this article will be shared on reasonable request to the corresponding author.

REFERENCES

- Abernethy F. A. J., Sheridan S., Barber S. J., 2020, *Planet. Space Sci.*, 180, 104784
- Anderson R. C. et al., 2012, *Space Sci. Rev.*, 170, 57
- Arslan, H., Batiste, S., Sture, S., 2010, *J. Aerosp. Eng.*, 23, 1
- Barber S. J. et al., 2018, *LPI Contrib.*, 2083, 2172
- Bergstrom J.S., Hilbert L. B., 2005, *Mech. Mater.*, 37, 899
- Calleja G., Jourdan A., Amedur B., Habas J.-P., 2013, *Eur. Polym. J.*, 49, 2214
- Colwell J. E., Batiste S., Horanyi M., Robertson S., Sture S., 2007, *Rev. Geophys.*, 45, RG2006
- Goesmann F., 2007, *Space Sci. Rev.*, 128, 257
- Grün E., Horanyi M., Sternovsky Z., 2011, *Planet. Space Sci.*, 59, 1672
- Hill, E., Mellin, M.J., Deane, B., Liu, Y., Taylor, L.A., 2007, *J. Geophys. Res.* 112, E02006
- Kennedy T., Mumm E., Myrick T., Frader-Thompson S., 2006, Proc. AIAA SPACE 2006 Conf. Exposition, #7402, Optimization of a Mars Sample Manipulation System Through Concentrated Functionality. AIAA SPACE Forum, USA
- LaMarch, C.Q., Curtis, J.S., Metzger, P.T., 2011, *Icarus*, 212, 383
- Li S., Milliken R. E., 2017, *Sci. Adv.*, 3, e1701471
- Lin H. et al., 2022, *Sci. Adv.*, 8, 9174
- Liu Y., Taylor L. A., 2011, *Planet. Space Sci.*, 1769
- Matteucci S., Yampolskii Y., Freeman B. D., Pinnau I., 2006, in Yampolskii Y., Pinnau I., Freeman B.D, eds, *Materials Science of Membranes for Gas and Vapor Separation*. John Wiley & Sons Ltd, New York, p. 1
- McCrum N. G., 1959, *J. Polym. Sci.*, 34, 355
- Moelle R. C., 2020, *Space Sci. Rev.*, 217, 5
- Morse A. D., Morgan G. H., Andrews D. J., Barber S. J., Leese M. R., Sheridan S., Wright I. P., Pillinger C. T., 2009, in Schulz R., Alexander C., Boehnhardt H., Glassmeier K., eds, *Rosetta: ESA’s Mission to the Origin of the Solar System*. Springer, New York, USA, p. 669
- Mortimer J., Verchovsky A. B., Anand M., 2016, *Geochim. Cosmochim. Acta*, 193, 36
- Mumm E., Roberts D., Kennedy T., Carlson L., Rutberg M., Ji J., 2008, Proc. AIAA SPACE 2008 Conf. Exposition, #7736, Sample Manipulation System for Sample Analysis at Mars. AIAA SPACE Forum, USA
- Pasternak R. A., Christensen M. V., Helle J., 1970, *Macromolecules*, 3, 366
- Rae P. J., Dattelbaum D. M., 2004, *Polymer*, 45, 7615
- Ray C. S., Reis S. T., Sen S., O’Dell J. S., 2010, *J. Non-Crystalline Solids*, 356, 2369
- Richter L., Carianni P., Durrant S., Hofmann P., Mühlbauer Q., Musso F., Paul R., Redlich D., 2015, Proc. ASTRA 2015, Progress Report on Development of the ExoMars 2018 Sample Processing and Distribution Subsystem (SPDS) and Related OHB Sample Handling Studies. ESTEC, Noordwijk
- Sargeant H. M., Barber S. J., Anand M., Abernethy F. A. J., Sheridan S., Wright I. P., Morse A. D., 2021, *Planet. Space Sci.*, 205, 105287
- Sebők B., Schülke M., Réti F., Kiss G., 2016, *Polym. Test.*, 49, 66
- Wright I. P. et al., 2007, *Space Sci. Rev.*, 128, 363
- Zheng X., Wen X., Wang W., Gao J., Ma L., Yu J., 2017, *Polym. Test.*, 60, 229

This paper has been typeset from a $\text{\TeX}/\text{\LaTeX}$ file prepared by the author.